Zygote

cambridge.org/zyg

Dynamic reprogramming and function of RNA N^6-methyladenosine modification during porcine early embryonic development

Tong Yu[1,*], Xin Qi[1,*], Ling Zhang[1,*], Wei Ning[1], Di Gao[1], Tengteng Xu[1], Yangyang Ma[1], Jason G Knott[2], Anucha Sathanawongs[3], Zubing Cao[1] and Yunhai Zhang[1]

[1]Anhui Province Key Laboratory of Local Livestock and Poultry, Genetical Resource Conservation and Breeding, College of Animal Science and Technology, Anhui Agricultural University, Hefei 230036, China; [2]Developmental Epigenetics Laboratory, Department of Animal Science, Michigan State University, East Lansing, MI 48824, USA and [3]Department of Veterinary Biosciences and Veterinary Public Health, Faculty of Veterinary Medicine, Chiang Mai University, A. Muang 50100, Thailand

Research Article

Cite this article: Yu T *et al*. (2021) Dynamic reprogramming and function of RNA N^6-methyladenosine modification during porcine early embryonic development. *Zygote*. **29**: 417–426. doi: 10.1017/S0967199420000799

Received: 20 September 2020
Revised: 25 November 2020
Accepted: 30 November 2020
First published online: 23 April 2021

Keywords:
Early embryos; m^{6}A; Nuclear transfer; Pig; Reprogramming

Authors for correspondence:
Yunhai Zhang and Zubing Cao. College of Animal Science and Technology, Anhui Agricultural University, Hefei 230036, China.
E-mail: yunhaizhang@ahau.edu.cn; zubingcao@ahau.edu.cn

*These authors contributed equally to this study.

Summary

N^6-Methyladenosine (m^{6}A) regulates oocyte-to-embryo transition and the reprogramming of somatic cells into induced pluripotent stem cells. However, the role of m^{6}A methylation in porcine early embryonic development and its reprogramming characteristics in somatic cell nuclear transfer (SCNT) embryos are yet to be known. Here, we showed that m^{6}A methylation was essential for normal early embryonic development and its aberrant reprogramming in SCNT embryos. We identified a persistent occurrence of m^{6}A methylation in embryos between 1-cell to blastocyst stages and m^{6}A levels abruptly increased during the morula-to-blastocyst transition. Cycloleucine (methylation inhibitor, 20 mM) treatment efficiently reduced m^{6}A levels, significantly decreased the rates of 4-cell embryos and blastocysts, and disrupted normal lineage allocation. Moreover, cycloleucine treatment also led to higher levels in both apoptosis and autophagy in blastocysts. Furthermore, m^{6}A levels in SCNT embryos at the 4-cell and 8-cell stages were significantly lower than that in parthenogenetic activation (PA) embryos, suggesting an abnormal reprogramming of m^{6}A methylation in SCNT embryos. Correspondingly, expression levels of m^{6}A writers (*METTL3* and *METTL14*) and eraser (*FTO*) were apparently higher in SCNT 8-cell embryos compared with their PA counterparts. Taken together, these results indicated that aberrant nuclear transfer-mediated reprogramming of m^{6}A methylation was involved in regulating porcine early embryonic development.

Introduction

Pigs are increasingly used as a dual-purpose model that benefits agricultural and biomedical research (Ireland *et al*., 2008; Perleberg *et al*., 2018). The agricultural and biomedical applications of pigs in gene editing, human disease models and stem cell research rely on a large number of SCNT embryos obtained *in vitro*. However, early developmental efficiency of SCNT embryos in pigs is still suboptimal compared with naturally fertilized embryos and cloned embryos from other species (Fowler *et al*., 2018; Yang *et al*., 2019; Wang *et al*., 2020). This is mainly due to an inadequate understanding of unique molecular mechanisms underlying porcine early embryonic development (Ramos-Ibeas *et al*., 2018). Accumulating evidence has indicated that removal and re-establishment of epigenetic information is an inherent hallmark of early embryonic development in mammals (Marcho *et al*., 2015; Canovas and Ross, 2016; Xu and Xie, 2018). Functional studies have indicated that writers and erasers for DNA and histone methylation play an essential role in preimplantation development of mammalian fertilized embryos (Lee *et al*., 2014; Huang *et al*., 2015; Fraser and Lin, 2016; Cheng *et al*., 2019). Abnormal expression of these epigenetic modifiers even severely hindered both genomic reprogramming of somatic cells and early development of SCNT embryos (Matoba and Zhang, 2018). Although epigenetic regulation of early embryonic development at the DNA and histone levels has been studied extensively, little information is known about the role of RNA modifications in early embryonic development.

N^6-Methyladenosine (m^{6}A) is the most prevalent RNA modification on eukaryotic message RNAs (mRNAs) (Nachtergaele and He, 2018). Recently, m^{6}A methylation was proved to be a reversible chemical modification that is deposited by methyltransferases (METTL3, METTL14 and WTAP) and removed by demethylases (FTO and ALKB5H), respectively (Shi *et al*., 2019). The m^{6}A modification has been shown to regulate many steps in RNA metabolism, such as stability, degradation, translation, splicing and localization (Huang *et al*., 2020). Accumulating studies have shown that m^{6}A modification in the animal

© The Author(s), 2021. Published by Cambridge University Press.

CAMBRIDGE UNIVERSITY PRESS

reproduction field has been implicated in a variety of cellular and physiological events including spermatogenesis (Lin *et al.*, 2017b), oogenesis (Hu *et al.*, 2020), germ cell maturation (Wang *et al.*, 2018; Xia *et al.*, 2018), maternal-to-zygotic transition (Zhao *et al.*, 2017; Hu *et al.*, 2020) and blastocyst formation (Kwon *et al.*, 2019). In addition, m^6A modification also plays a critical role in pluripotency maintenance, differentiation of embryonic stem cells (ESCs) (Wang *et al.*, 2014), and reprogramming of somatic cells into pluripotent stem cells (Chen *et al.*, 2015). It is worth noting that inconsistent results on the function of m^6A modification in maintenance and differentiation of ESCs have been manifested in different studies (Park and Hong, 2017). Similarly, m^6A modification also exhibited stimulatory and inhibitory effects on transcription factor-mediated somatic reprogramming (Guo *et al.*, 2017). However, the role of m^6A modification in porcine early embryonic development and its characteristics in nuclear transfer-mediated somatic reprogramming remain unclear.

In the present study, we identified a persistent occurrence of m^6A methylation in porcine early embryos. Using a pharmacological approach, we demonstrated that m^6A modification is indispensable for both early embryonic development and lineage allocation. Furthermore, m^6A methylation exhibited an aberrant reprogramming in porcine early cloned embryos. Our findings provide new insights into epitranscriptomic regulation of early embryonic development and nuclear transfer-mediated somatic reprogramming.

Materials and methods

All chemicals in this study were purchased from Sigma (Sigma-Aldrich, St Louis, MO) unless otherwise stated.

Preparation of methylation inhibitor cycloleucine

Cycloleucine (Sigma, HY-19160) was dissolved in porcine zygote medium (PZM-3) to make 80 mM stock solutions. Then, the stock was further diluted using PZM-3 to obtain the desired working solution (10 mM, 20 mM and 40 mM).

Oocyte in vitro maturation

Ovaries were collected from gilts at a local slaughterhouse and follicular fluid was aspirated from antral follicles at 3–6 mm in diameter. Cumulus–oocyte complexes (COCs) were selected under a stereomicroscope. Subsequently, COCs were cultured in one well of 4-well plate containing 400 µl of *in vitro* maturation medium (TCM-199 supplemented with 5% FBS, 10% porcine follicular fluid, 10 IU/ml eCG, 5 IU/ml hCG, 100 ng/ml L-cysteine, 10 ng/ml EGF, 0.23 ng/ml melatonin, 2.03×10^{-5} ng/ml LIF, 2×10^{-5} ng/ml IGF-1, 4×10^{-5} ng/ml FGF2, 100 U/ml penicillin and 100 mg/ml streptomycin) for 44 h at 38.5°C, 5% CO_2 and saturated humidity. Cumulus cells surrounding oocytes were removed using 1 mg/ml hyaluronidase following maturation.

Parthenogenetic activation (PA)

Metaphase II (MII) oocytes were stimulated using two pulses of direct current (1.56 kV/cm for 80 ms) in activation medium (0.3 M mannitol supplemented with 0.1 mM $CaCl_2$, 0.1 mM $MgCl_2$ and 0.01% polyvinyl alcohol). Subsequently, activated oocytes were washed with PZM-3 and were incubated in chemically assisted activation medium (PZM-3 supplemented with 10 µg/ml cycloheximide and 10 µg/ml cytochalasin B) for 4 h. Then, embryos were cultured in PZM-3 droplets at 38.5°C, in 5% CO_2 and 95% air with saturated humidity.

Somatic cell nuclear transfer

Donor cells and oocytes were placed in the operation medium TCB (TCM-199 with 7.5 mg/l cytochalasin B and 2% fetal bovine serum). The oocytes were enucleated by blind suction method, and a single donor cell was injected into the enucleated cytoplasm. The reconstructed oocytes were restored in PZM-3 droplets for 30 min. Then, the somatic cells and oocytes were fused using a direct current pulse (1.56 kV/cm for 100 ms) and further activated with chemical-assisted activation solution for 4 h. The fused embryos were cultured in PZM-3 droplets at 38.5°C, in 5% CO_2 and 95% air with saturated humidity.

Real-time quantitative PCR

Total RNAs were extracted from oocytes and embryos using the RNeasy Mini Kit (Qiagen, 74104). The RNA was quantified by spectrophotometry at A_{260}/A_{280} nm on a NanoDrop 2000 instrument (Thermo Scientific, Waltham, MA, USA). Reverse transcription was immediately performed using a QuantiTect Reverse Transcription Kit (Qiagen, 205311). The cDNA was aliquoted and stored at −80 °C until ready for use. The primers used in the present study are listed in Table 1. The assembly for polymerase chain reaction (PCR) was prepared in the FastStart SYBR Green Master mix (Roche, 04673514001) and was run on a StepOne Plus (Applied Biosystems, Foster, USA). The following qPCR procedures were performed: predenaturation at 95°C for 10 min, followed by 45 amplification cycles of 95°C denaturation for 15 s, 60°C annealing for 10 s, and 72°C extension for 20 s. The quantification cycle (Cq) samples for each target gene were normalized to the value of the *EF1α1* mRNA transcript. qPCR was performed in triplicate to minimize variations in operator techniques. The Cq values were obtained and transferred to a Microsoft Excel spreadsheet for further relative quantification analysis using the $2^{-\Delta\Delta Ct}$ method. The samples were collected three times and three biological replicates were collected for each gene.

Immunofluorescence staining

Oocytes or embryos were fixed in 4% paraformaldehyde (PFA) solution for 15 min, permeabilized with 1% Triton X-100 in Dulbecco's phosphate-buffered saline (DPBS) for 30 min at room temperature (RT) and then blocked with 2% BSA in DPBS at RT for 1 h. Samples were incubated overnight at 4°C in blocking solution containing primary antibodies. The detailed information regarding primary antibodies used is listed in Table 2. Following several washes, samples were incubated in the dark at 37°C for 1 h in blocking solution containing secondary antibodies. After washing, samples were counterstained for 10 min in 4,6-diamidino-2-phenylindole dihydrochloride (DAPI) or propidium iodide (PI) solution and were then loaded onto glass slides and covered with a glass coverslip. Finally, samples were imaged under an inverted fluorescence microscope (Olympus, Japan). The average pixel intensity of embryos was determined using ImageJ software.

https://doi.org/10.1017/S0967199420000799 Published online by Cambridge University Press

Table 1. Porcine-specific primer sequences used in this study

Gene symbol	Primer sequences (5′→3′)	Product size (bp)	GenBank accession number
METTL3	F: CTGGGGTTACGAACGGGTAG	125	XM_003128580.5
	R: TGACACCAACCAAGCAGTGT		
METTL14	F: GGGAGAGTGTGTTTACGCAAGTG	145	XM_003129231.6
	R: TTCCCATAAGGCAGTGTTCCTT		
WTAP	F: CTGCACGCAGGGAAAACAT	140	XM_005659114.3
	R: TGGGTCGACCATTGTTGATCT		
FTO	F: AGAATGTCCGTGATGAGGCG	110	NM_001112692.1
	R: CAGCAACTCACACTCGACCC		
ALKBH5	F: CAACAGCGCCGTCATCAAC	150	XM_021067995.1
	R: ATAGGCTTGAACTGGAACTTGCA		
OCT4 (*POU5F1*)	F: CGAGAACCGAGTGAGAGG	206	NM_001113060.1
	R: GGAAAGGAGACCCAGCAG		
SOX2	F: CGCAGACCTACATGAACG	103	NM_001123197.1
	R: TCGGACTTGACCACTGAG		
CDX2	F: AGTCGCTACATCACCATTCGGAG	139	NM_001278769.1
	R: GCTGCTGTTGCTGCAACTTCTTC		
NANOG	F: CTCTCCTCTTCCTTCCTC	139	NM_001129971.1
	R: CTTCTGCTTCTTGACTGG		
TEAD4	F: CATTACTCCTACCGCATCC	151	NM_001142666.1
	R: CCTGTGTGTCTCTGTTGG		
GATA3	F: CACGACACGCTGGAGGAC	106	NM_001044567.1
	R: GGCTGGAGTGGCTGAAGG		
EOMES	F: CCATCTCCCACGGATTCTCC	133	XM_005669315.3
	R: GCACGGTTCTCTCGCCATTA		
BMP4	F: GGCTGACCACCTCAACTCAA	102	NM_001101031
	R: CTCAGTTCGGTGGGAACACA		
TFAP2C	F: CACGTTCCGGTTGAAAAGGC	105	NM_001123201.1
	R: CAGTCCAGGGTTTCGGAGAG		
ELF5	F: CTCTTGCCTTGAAAACCTCCTC	131	NM_001243711
	R: ACAGGTCGGTCCACGACATC		
EF1α1	F: ATTGTTGCTGCTGGTGTTG	161	NM_001097418–2
	R: TCATATCTCTTCTGGCTGTAGG		

F: forward; R: reverse.

Terminal deoxynucleotidyl transferase (TdT)-mediated dUDP nick-end (TUNEL) staining

Blastocysts were fixed in 4% PFA for 15 min at RT. Following several washes, blastocysts were incubated in DNase I (TIANGEN, RT411, China) for 1 h at 38.5°C. After washing, blastocysts treated with label solution (*In Situ* Cell Death Detection Kit, 7791-13-1, Roche, Germany) served as the negative control group. Blastocysts treated with enzyme solution served as the positive control group. Blastocysts without DNase I treatment from other groups were incubated directly in enzyme solution for 1 h. All blastocysts were stained with DAPI for 15 min and were then imaged using laser scanning confocal microscopy (Olympus, Japan). Total numbers of cells and numbers of apoptotic dead cells were counted and the apoptotic ratio was calculated by dividing the number of dead cells by the total number of cells, which included dead cells.

Statistical analysis

All experiments were carried out at least three times. The data were analyzed using one-way analysis of variance (ANOVA) or Student's *t*-test (SPSS 17.0) and were presented as mean ± standard error of the mean (mean ± SEM). A P-value < 0.05 was considered to be statistically significant.

https://doi.org/10.1017/S0967199420000799 Published online by Cambridge University Press

Table 2. Antibodies used in this study

Information on primary antibodies used in this study			
Primary antibody	Species	Vendor	Cat. no. and dilution
m^6A	Rabbit	Abcam	ab190866 (1:75)
CDX2	Mouse	Biogenex	AM392 (ready to use)
LC3B	Rabbit	Cell Signalling	2775S (1:200)
Information on secondary antibodies used in this study			
Secondary antibody	Species	Vendor	Cat. no. and dilution
Alexa Fluor 488 anti-mouse IgG	Goat	Invitrogen	A11029 (1:200)
Alexa Fluor 488 anti-rabbit IgG	Goat	Invitrogen	A11008 (1:200)
Alexa Fluor 594 anti-rabbit IgG	Goat	Invitrogen	A11012 (1:200)

Results

Cycloleucine treatment impaired developmental competence and quality of porcine early embryos

To explore the role of m^6A methylation in porcine early embryonic development, embryos at the pronuclear stage were cultured for 7 days in medium containing different concentrations of cycloleucine. The results revealed that treatment with 10 mM cycloleucine did not affect the rates of 4-cell stage embryos (81.67 ± 8.81% vs. 63.33 ± 8.33%), 8-cell stage embryos (65.00 ± 7.64% vs. 55.00 ± 8.66%), morula (65.00 ± 7.64% vs. 55.00 ± 8.66%) and blastocysts (56.67 ± 6.67% vs. 43.33 ± 3.33%) (Fig. 1A–E). Treatment with cycloleucine (40 mM and 80 mM) significantly reduced the rates of 4-cell stage embryos (81.67 ± 8.81% vs. 38.33 ± 6.01%, 16.67 ± 4.41%), 8-cell stage embryos (65.00 ± 7.64% vs. 15.00 ± 2.88%, 1.67 ± 1.67%), morula (65.00 ± 7.64% vs. 6.67 ± 1.67%, 1.67 ± 1.67%) and blastocysts (56.67 ± 6.67% vs. 6.67 ± 1.67%, 0.00 ± 0.00%) (Fig. 1A–E) ($P < 0.05$). Interestingly, treatment with 20 mM cycloleucine only significantly decreased the rates of 4-cell stage embryos (81.67 ± 8.81% vs. 50.00 ± 10.40%) (Fig. 1B) and blastocysts (56.67 ± 6.67% vs. 26.67 ± 6.67%) (Fig. 1A, E) ($P < 0.05$), but did not affect development to the 8-cell stage embryos (65.00 ± 7.64% vs. 46.67 ± 11.67%) and morula (65.00 ± 7.64% vs. 46.67 ± 11.67%) (Fig. 1C, D). Furthermore, there were no blastocysts in the high dosage cycloleucine treatment groups (40 mM and 80 mM), while a small portion of blastocysts was still present in the 20 mM cycloleucine treatment group (Fig. 1A). Therefore, the 20 mM cycloleucine concentration was used in subsequent experiments. To analyze lineage allocation of trophectoderm (TE) and inner cell mass (ICM), blastocysts were stained with CDX2 to determine the TE cell number (Fig. 1F). The number of ICM cells was indirectly determined by subtracting the TE number from the total cell number. We found that the ICM cell number did not change between control and treatment groups (12.89 ± 1.15 vs. 12.63 ± 0.79) (Fig. 1G). However, cycloleucine treatment led to a significant reduction in the number of total cells (43.67 ± 3.09 vs. 29.15 ± 1.75) and TE cells (30.78 ± 2.71 vs. 16.52 ± 1.86) (Fig. 1G) ($P < 0.05$). Moreover, the ratio of ICM cells to TE cells in blastocysts in the treatment group significantly increased compared with the control group (0.53 ± 0.08 vs.1.08 ± 0.13) (Fig. 1G) ($P < 0.05$). Altogether, these data demonstrated that cycloleucine treatment was detrimental to early embryonic development and normal lineage allocation in pigs.

Cycloleucine treatment decreased m^6A modification levels in porcine early embryos

To investigate whether cycloleucine treatment affected m^6A levels in embryos, immunofluorescence staining of 4-cell embryos (Fig. 2A) and blastocysts (Fig. 2C) was performed to analyze signal intensity of m^6A. The results showed that cycloleucine treatment significantly reduced m^6A levels in 4-cell embryos and blastocysts compared with the control group (Fig. 2B, D) ($P < 0.05$). To determine whether cycloleucine treatment affected the expression of genes associated with ICM and TE lineage specification, blastocysts were subject to qPCR analyses. The results showed that there was no change in expression levels of several genes between control and treatment groups, while cycloleucine treatment resulted in a significant reduction in *TFAP2C* expression levels (Fig. S1) ($P < 0.05$). Therefore, these results suggested that cycloleucine treatment effectively reduced m^6A modification levels in porcine early embryos.

Reduced m^6A methylation levels increased apoptosis and autophagy in porcine blastocysts

To study whether reduced m^6A levels affected expression of genes associated with apoptosis and autophagy, blastocysts were subject to qPCR analyses. The results revealed that there were no changes in expression of genes including *ATG5*, *BECL1N1*, *CASPASE3*, *BAX* and *P53* between control and treatment groups (Fig. 3A). However, cycloleucine treatment significantly decreased the expression of anti-apoptotic gene *BCL2*, and increased the expression of autophagy gene *LC3* (Fig. 3A) ($P < 0.05$). Furthermore, TUNEL staining showed that cycloleucine treatment did not affect the number of TUNEL-positive cells (Fig. 3B, C), but resulted in a higher apoptosis ratio in blastocysts (Fig. 3B, D) ($P < 0.05$). Immunofluorescence analyses revealed that cycloleucine treatment significantly enhanced the expression levels of LC3 protein in blastocysts (Fig. 3E, F) ($P < 0.05$). Therefore, our data indicated that reduction of m^6A levels increased apoptosis and autophagy in porcine blastocysts.

Aberrant reprogramming of m^6A methylation during early development of porcine cloned embryos

To elucidate the dynamic reprogramming of m^6A modification in PA and SCNT embryos, immunofluorescence staining of embryos

https://doi.org/10.1017/S0967199420000799 Published online by Cambridge University Press

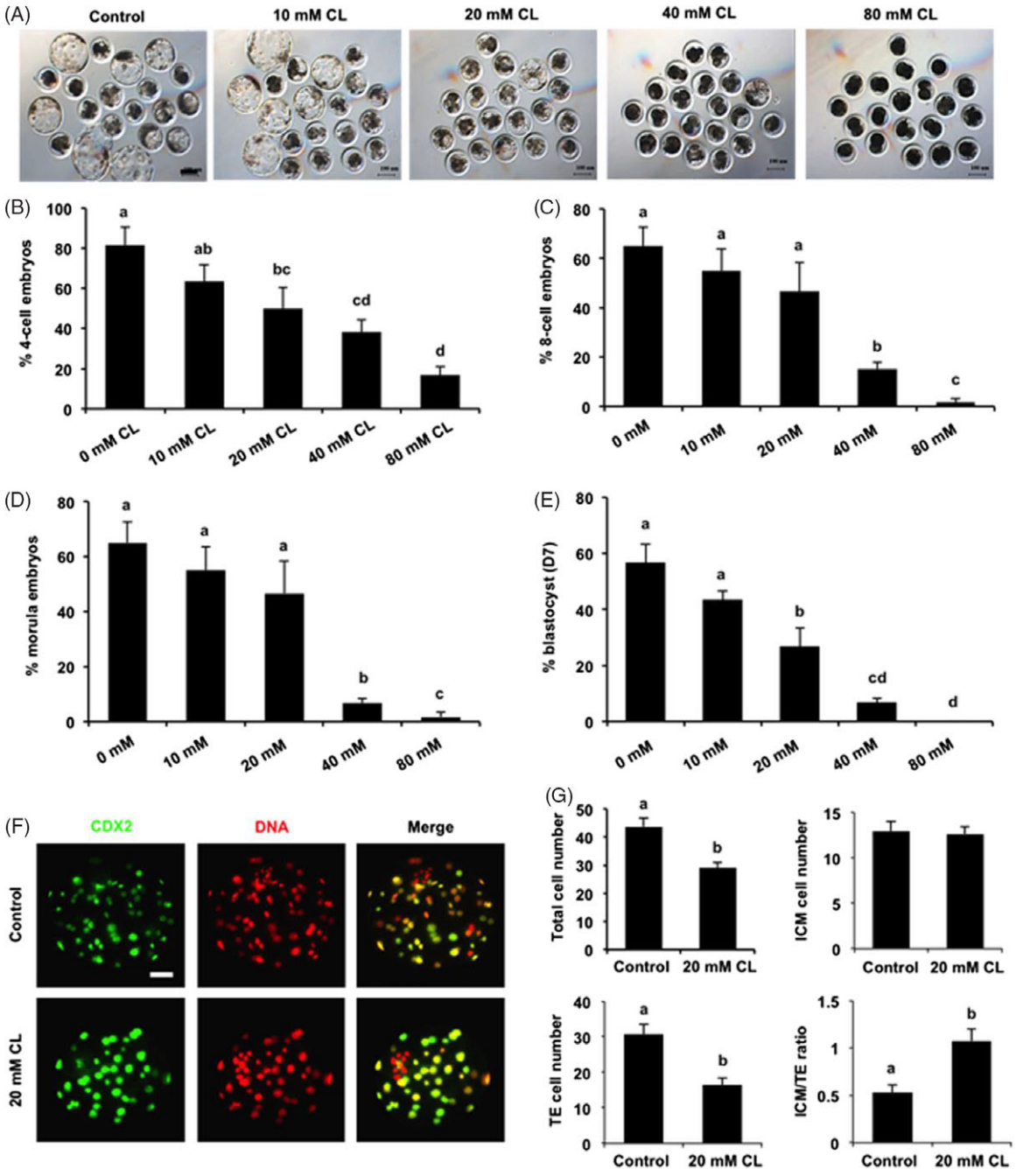


Figure 1. Effects of different concentrations of cycloleucine on porcine early embryonic development and quality. (*A*) Representative images of blastocysts in each group. Blastocysts from control and CL treatment group were imaged. CL, cycloleucine. Scale bars: 100 μm. Developmental rates of embryos at the 4-cell (*B*), 8-cell (*C*), morula (*D*) and blastocyst stage (*E*). The developmental rates of embryos in each group were recorded and statistically analyzed. (*F*) Immunofluorescence staining of blastocysts. Representative images obtained using confocal microscopy are shown. The experiment was independently repeated three times with at least 20 blastocysts per group. Scale bar: 50 μm. (*G*) Lineage allocation analysis of blastocysts from the control and CL treatment group. Total cell numbers, ICM cells, TE cells, and the ratio of ICM cells to TE cells were separately recorded and were subjected to statistical analysis. ICM: inner cell mass; TE: trophectoderm. All data are represented as mean ± SEM and different letters on the bars indicate significant differences ($P < 0.05$).

at different developmental stages was performed to detect signal intensity of m^{6}A modification (Fig. 4A). Immunofluorescence analyses revealed that m^{6}A methylation was present in the cytoplasm of PA embryos between 1-cell to blastocyst stages and m^{6}A levels significantly increased during the morula-to-blastocyst transition (Fig. 4A, B). There were no significant differences in m^{6}A levels in 2-cell, morula and blastocysts between PA and SCNT (Fig. 4A, B). However, m^{6}A levels in SCNT 1-cell embryos were significantly higher than that in their PA counterparts (Fig. 4A, B) ($P < 0.05$). In contrast, m^{6}A levels in SCNT 4-cell

https://doi.org/10.1017/S0967199420000799 Published online by Cambridge University Press

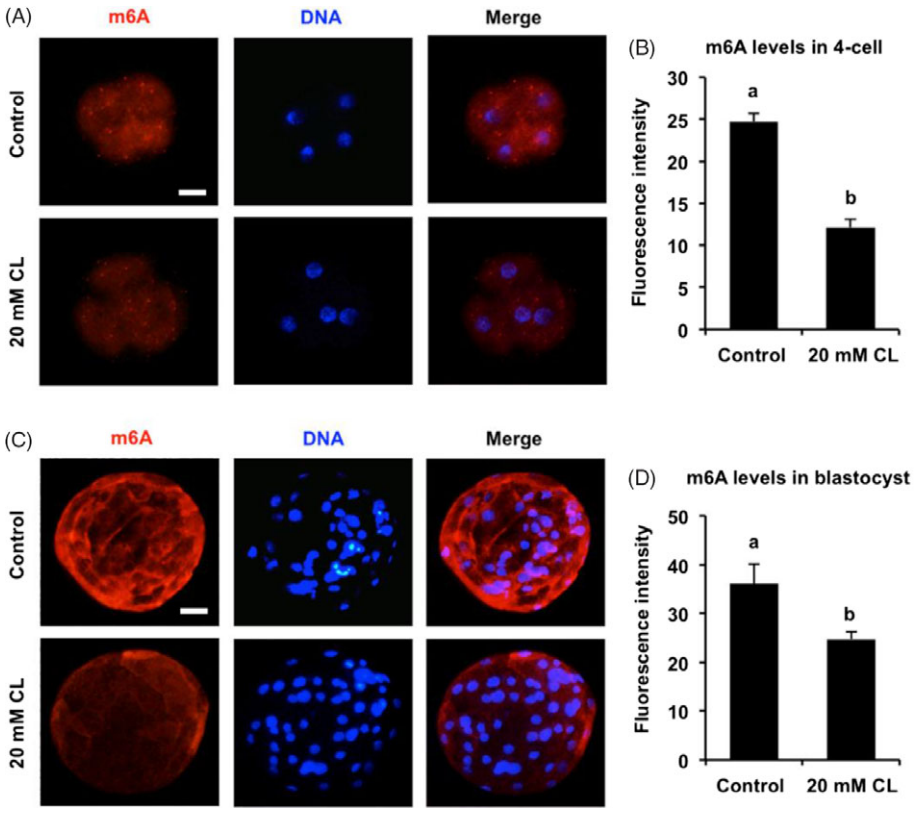


Figure 2. Effect of cycloleucine treatment on m^{6}A modification levels in porcine early embryos. (*A*) Immunofluorescence staining of 4-cell embryos. Representative images obtained using confocal microscopy are shown. The experiment was independently repeated three times with at least 30 embryos per group. Scale bar: 50 μm. (*B*) Quantitative analysis of m^{6}A levels in 4-cell embryos. (*C*) Immunofluorescence staining of blastocysts. Representative images are shown. The experiment was independently repeated three times with at least 24 embryos per group. Scale bar: 50 μm. (*D*) Quantitative analysis of m^{6}A levels in blastocysts. All data are presented as mean ± SEM and different letters on the bars indicate significant differences ($P < 0.05$).

and 8-cell embryos were apparently lower than that in PA counterparts (Fig. 4A, B) ($P < 0.05$). Therefore, these results demonstrated that m^{6}A methylation exhibited an aberrant reprogramming in porcine SCNT embryos.

Abnormal expression of genes encoding m^{6}A writers and erasers in porcine early cloned embryos

To further determine the relative expression levels of genes encoding m^{6}A writers and erasers between PA and SCNT embryos, qPCR was performed to address the question. We found that expression levels of *METTL3*, *METTL14*, *FTO* and *WTAP* in SCNT 4-cell embryos were similar to that in their PA counterparts (Fig. 5A). However, *ALKB5H* mRNA levels in SCNT 4-cell embryos were significantly lower than that in PA 4-cell embryos (Fig. 5A) ($P < 0.05$). Additionally, at the 8-cell stage, expression levels of *METTL3*, *METTL14* and *FTO* in SCNT embryos were significantly higher than that in PA embryos (Fig. 5B) ($P < 0.05$), while there was no significant difference in expression levels of *WTAP* and *ALKB5H* between PA and SCNT embryos (Fig. 5B). Therefore, these data indicated that genes encoding m^{6}A writers and erasers displayed an abnormal expression in porcine SCNT embryos.

Discussion

Despite the essential role of m^{6}A methylation in porcine oocyte maturation being demonstrated (Wang *et al.*, 2018), the role of m^{6}A modification in early embryonic development and dynamics of m^{6}A reprogramming in SCNT embryos remains unknown. Here our results showed that m^{6}A modification is required for porcine early embryonic development, while it exhibited an aberrant reprogramming pattern in SCNT embryos. To our knowledge, the reprogramming pattern of m^{6}A modification was characterized here for the first time in SCNT embryos.

Establishment of the functional TE lineage is an essential prerequisite for mammalian blastocyst formation (Choi *et al.*, 2012; Posfai *et al.*, 2019). Proliferation and differentiation of TE cells is accompanied by the establishment of a functional TE lineage. In this study, we found that reduced m^{6}A levels induced by cycloleucine treatment significantly decreased TE cell numbers. It is therefore possible that m^{6}A modification mediated TE proliferation and differentiation to allow blastocyst formation in pigs. Conversely, our data showed that expression of anti-apoptotic gene *BCL2* and apoptosis ratio significantly increased in cycloleucine-treated blastocysts. Previous studies have indicated that increased apoptosis ratio frequently impaired the formation of both TE cells and blastocyst (Lin *et al.*, 2017a). In addition, reduced m^{6}A levels also resulted in a higher level of autophagy in porcine blastocysts. One study indicated that induction of autophagy resulted in defects in TE cell differentiation in mice (Lee *et al.*, 2011), and excessive levels of autophagy were detrimental to blastocyst development (Kim *et al.*, 2017; Song *et al.*, 2014). Therefore, we speculated that high levels of apoptosis and autophagy induced by cycloleucine might inhibit TE cell

https://doi.org/10.1017/S0967199420000799 Published online by Cambridge University Press

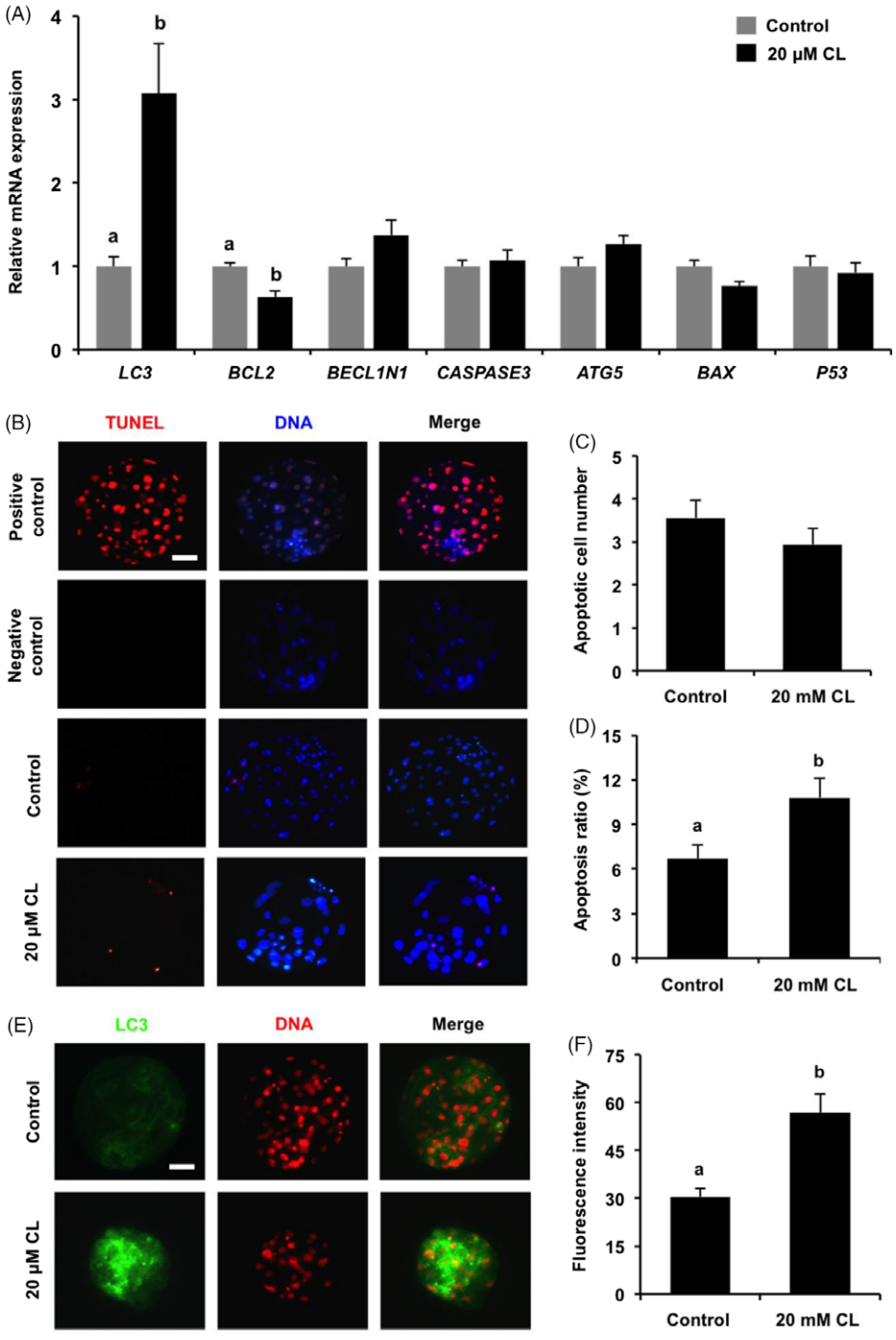


Figure 3. Effect of cycloleucine treatment on apoptosis and autophagy in porcine blastocysts. (*A*) Effect of cycloleucine treatment on expression of genes associated with apoptosis and autophagy. The relative abundance of mRNA of the indicated genes in blastocysts in each group was determined by qPCR. (*B*) TUNEL staining in blastocysts. Red spots indicate apoptotic cells, blue spots mark nuclei. Representative images obtained by confocal microscopy are shown. Scale bar: 50 μm. (*C*) Analyses of number cells TUNEL-positive in blastocysts. (*D*) Analyses of apoptosis ratio in blastocysts. (*E*) Immunofluorescence staining of LC3 protein. Blastocysts in each group were stained for LC3 and DNA. The experiment was independently repeated three times with at least 25 blastocyst per group. Scale bar: 50 μm. (*F*) Quantitative analysis of LC3 protein levels in blastocysts. All data are shown as mean ± SEM and different letters on the bars indicate significant differences ($P < 0.05$).

proliferation and differentiation, thereby impeding blastocyst formation.

Epigenetic reprogramming of chromatin after fertilization allows zygotic genome activation (ZGA) and development to full term (Fraser and Lin, 2016; Xu and Xie, 2018). Aberrant epigenetic reprogramming is closely related to poor developmental competence in fertilized embryos and somatic cloned embryos (Shi and Haaf, 2002; Matoba and Zhang, 2018). Recently, m^6A modification was reported to regulate ZGA in zebrafish (Zhao *et al.*, 2017) and mice (Hu *et al.*, 2020). Our results in this study showed that reduced m^6A levels induced by cycloleucine treatment caused developmental arrest at the 4-cell stage. In pigs, ZGA mainly occurs at the 4-cell stage (Zhou *et al.*, 2020). Therefore, it is likely that m^6A modification mediates ZGA to sustain normal development of 4-cell embryos.

Natural reprogramming of epitranscriptomic modifications during ZGA under the physiological context provides a reliable reference for artificial reprogramming in SCNT embryos

https://doi.org/10.1017/S0967199420000799 Published online by Cambridge University Press

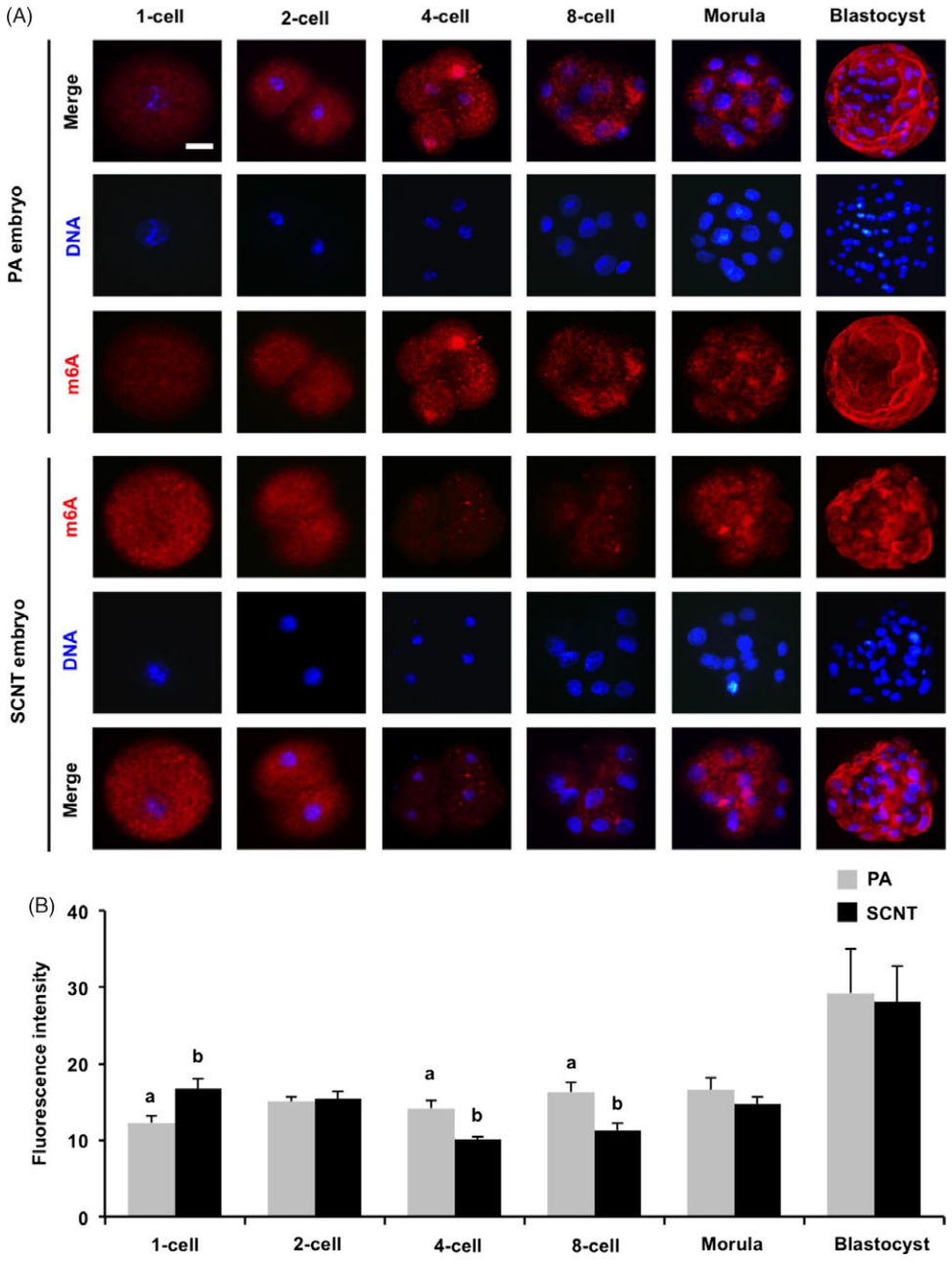


Figure 4. Dynamic reprogramming of m^{6}A methylation during early development of porcine cloned embryos. (*A*) Immunofluorescence staining of embryos derived from PA and SCNT. Embryos at the indicated developmental stages were stained for m^{6}A (red) and DNA (blue). The experiment was independently repeated three times with at least 30 embryos per stage. Scale bar: 50 μm. (*B*) Quantitative analysis of m^{6}A levels in embryos derived from PA and SCNT. All data are shown as mean ± SEM and different letters on the bars indicate significant differences ($P < 0.05$).

(Yartseva and Giraldez, 2015). Reprogramming patterns of m^{6}A modification were characterized in detail during early development of porcine PA and SCNT embryos. Results indicated that m^{6}A levels were significantly increased in 1-cell cloned embryos, whereas they dramatically decreased in 4-cell and 8-cell embryos compared with PA embryos, suggesting an aberrant reprogramming of m^{6}A modification in porcine SCNT embryos. Correspondingly, genes encoding m^{6}A writers and erasers also exhibited an abnormal expression in cloned embryos, which might be used to explain the aberrant reprogramming of m^{6}A modification. In addition, previous studies have indicated that m^{6}A methylation facilitated or inhibited transcription factor-mediated somatic reprogramming (Wu *et al.*, 2019), suggesting that m^{6}A methylation indeed functions in somatic reprogramming. Therefore, functional research on m^{6}A methylation in nuclear transfer-mediated somatic reprogramming would be warranted in the future.

In conclusion, our results showed that m^{6}A methylation is essential for early embryonic development in pigs and exhibits an aberrant reprogramming in SCNT embryos. These findings provide new insights into the function of m^{6}A modification in mammalian preimplantation embryonic development.

https://doi.org/10.1017/S0967199420000799 Published online by Cambridge University Press

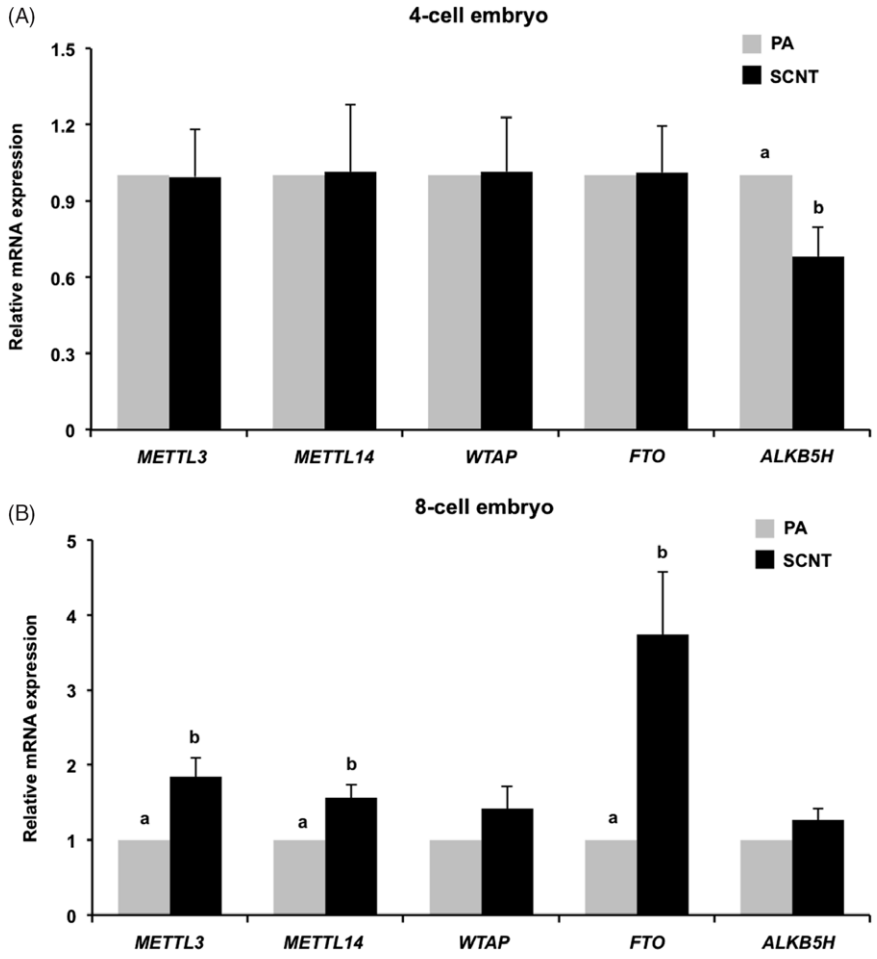


Figure 5. Expression of genes encoding m^{6}A writers and erasers in porcine PA and SCNT embryos. (*A*) Expression of genes in 4-cell embryos derived from PA and SCNT. (*B*) Expression of genes in 8-cell embryos derived from PA and SCNT. The relative abundance of *METTLE3*, *METTL14*, *WTAP*, *FTO and ALKB5H* mRNA was determined by qPCR. All data are shown as mean ± SEM and different letters on the bars indicate significant differences ($P < 0.05$).

Supporting information. Supporting information is available for this article at the publisher's website.

Ethical standards. All experiments were conducted in accordance with the Institutional Animal Care and Use Committee (IACUC) guidelines under currently approved protocols at Anhui Agricultural University.

Financial support. This work was supported by grants from the Anhui Provincial Natural Science Foundation (1908085MC97), the Science and Technology Major Project of Anhui province (18030701185 and 17030701061), the National Natural Science Foundation of China (31802059 and 31902226), the Hefei Innovation and Entrepreneurship Support Plan for Returnee Scholar, and the Anhui Provincial Innovation and Entrepreneurship Support Plan for Returnee Scholar (2020LCX015).

Authors contribution. ZC, JGK, and YZ conceived the project and wrote the manuscript. TY, XQ, LZ, WN, DG and TX performed the experiments. JGK and AS analyzed the data. All authors read and approved the final manuscript.

Conflict of interest. The authors declare no conflicts of interest with regard to the study.

Supplementary material. To view supplementary material for this article, please visit https://doi.org/10.1017/S0967199420000799

References

Canovas S and Ross PJ (2016). Epigenetics in preimplantation mammalian development. *Theriogenology* **86**, 69–79.

Chen T, Hao YJ, Zhang Y, Li MM, Wang M, Han W, Wu Y, Lv Y, Hao J, Wang L, Li A, Yang Y, Jin KX, Zhao X, Li Y, Ping XL, Lai WY, Wu LG, Jiang G, Wang HL, Sang L, Wang XJ, Yang YG and Zhou Q (2015). m^{6}A RNA methylation is regulated by microRNAs and promotes reprogramming to pluripotency. *Cell Stem Cell* **16**, 289–301.

Cheng H, Zhang J, Zhang S, Zhai Y, Jiang Y, An X, Ma X, Zhang X, Li Z and Tang B (2019). Tet3 is required for normal *in vitro* fertilization preimplantation embryos development of bovine. *Mol Reprod Dev* **86**, 298–307.

Choi I, Carey TS, Wilson CA and Knott JG (2012). Transcription factor AP-2gamma is a core regulator of tight junction biogenesis and cavity formation during mouse early embryogenesis. *Development* **139**, 4623–32.

Fowler KE, Mandawala AA, Griffin DK, Walling GA and Harvey SC (2018). The production of pig preimplantation embryos *in vitro*: current progress and future prospects. *Reprod Biol* **18**, 203–11.

Fraser R and Lin CJ (2016). Epigenetic reprogramming of the zygote in mice and men: on your marks, get set, go! *Reproduction* **152**, R211–22.

Guo M, Liu X, Zheng X, Huang Y and Chen X (2017). m^{6}A RNA modification determines cell fate by regulating mRNA degradation. *Cell Reprogram* **19**, 225–31.

Hu Y, Ouyang Z, Sui X, Qi M, Li M, He Y, Cao Y, Cao Q, Lu Q, Zhou S, Liu L, Shen B, Shu W and Huo R (2020). Oocyte competence is maintained by m^{6}A methyltransferase KIAA1429-mediated RNA metabolism during mouse follicular development. *Cell Death Differ* **27**, 2468–83.

Huang H, Weng H and Chen J (2020). The biogenesis and precise control of RNA m^{6}A methylation. *Trends Genet* **36**, 44–52.

Huang J, Zhang H, Wang X, Dobbs KB, Yao J, Qin G, Whitworth K, Walters EM, Prather RS and Zhao J (2015). Impairment of preimplantation

porcine embryo development by histone demethylase KDM5B knockdown through disturbance of bivalent H3K4me3-H3K27me3 modifications. *Biol Reprod* **92**, 72.

Ireland JJ, Roberts RM, Palmer GH, Bauman DE and Bazer FW (2008). A commentary on domestic animals as dual-purpose models that benefit agricultural and biomedical research. *J Anim Sci* **86**, 2797–805.

Kim MG, Kim DH, Lee HR, Lee JS, Jin SJ and Lee HT (2017). Sirtuin inhibition leads to autophagy and apoptosis in porcine preimplantation blastocysts. *Biochem Biophys Res Commun* **488**, 603–8.

Kwon J, Jo YJ, Namgoong S and Kim NH (2019). Functional roles of hnRNPA2/B1 regulated by METTL3 in mammalian embryonic development. *Sci Rep* **9**, 8640.

Lee K, Hamm J, Whitworth K, Spate L, Park KW, Murphy CN and Prather RS (2014). Dynamics of TET family expression in porcine preimplantation embryos is related to zygotic genome activation and required for the maintenance of NANOG. *Dev Biol* **386**, 86–95.

Lee SE, Hwang KC, Sun SC, Xu YN and Kim NH (2011). Modulation of autophagy influences development and apoptosis in mouse embryos developing *in vitro*. *Mol Reprod Dev* **78**, 498–509.

Lin T, Lee JE, Oqani RK, Kim SY, Cho ES, Jeong YD, Baek JJ and Jin DI (2017a). Delayed blastocyst formation or an extra day culture increases apoptosis in pig blastocysts. *Anim Reprod Sci* **185**, 128–39.

Lin Z, Hsu PJ, Xing X, Fang J, Lu Z, Zou Q, Zhang KJ, Zhang X, Zhou Y, Zhang T, Zhang Y, Song W, Jia G, Yang X, He C and Tong MH (2017b). Mettl3-/Mettl14-mediated mRNA N^6-methyladenosine modulates murine spermatogenesis. *Cell Res* **27**, 1216–30.

Marcho C, Cui W and Mager J (2015). Epigenetic dynamics during preimplantation development. *Reproduction* **150**, R109–20.

Matoba S and Zhang Y (2018). Somatic cell nuclear transfer reprogramming: mechanisms and applications. *Cell Stem Cell* **23**, 471–85.

Nachtergaele S and He C (2018). Chemical modifications in the life of an mRNA transcript. *Ann Rev Genet* **52**, 349–72.

Park CH and Hong K (2017). Epitranscriptome: m^6A and its function in stem cell biology. *Genes Genome* **39**, 371–8.

Perleberg C, Kind A and Schnieke A (2018). Genetically engineered pigs as models for human disease. *Dis Model Mech* 11, dmm030783.

Posfai E, Rovic I and Jurisicova A (2019). The mammalian embryo's first agenda: making trophectoderm. *Int J Dev Biol* **63**, 157–70.

Ramos-Ibeas P, Nichols J and Alberio R (2018). States and origins of mammalian embryonic pluripotency *in vivo* and in a dish. *Curr Top Dev Biol* **128**, 151–79.

Shi H, Wei J and He C (2019). Where, when, and how: context-dependent functions of RNA methylation writers, readers, and erasers. *Mol Cell* **74**, 640–50.

Shi W and Haaf T (2002). Aberrant methylation patterns at the two-cell stage as an indicator of early developmental failure. *Mol Reprod Dev* **63**, 329–34.

Song BS, Kim JS, Kim YH, Sim BW, Yoon SB, Cha JJ, Choi SA, Yang HJ, Mun SE, Park YH, Jeong KJ, Huh JW, Lee SR, Kim SH, Kim SU and Chang KT (2014). Induction of autophagy during *in vitro* maturation improves the nuclear and cytoplasmic maturation of porcine oocytes. *Reprod Fertil Dev* **26**, 974–81.

Wang X, Qu J, Li J, He H, Liu Z and Huan Y (2020). Epigenetic reprogramming during somatic cell nuclear transfer: recent progress and future directions. *Front Genet* **11**, 205.

Wang Y, Li Y, Toth JI, Petroski MD, Zhang Z and Zhao JC (2014). N6-methyladenosine modification destabilizes developmental regulators in embryonic stem cells. *Nat Cell Biol* **16**, 191–8.

Wang YK, Yu XX, Liu YH, Li X, Liu XM, Wang PC, Liu S, Miao JK, Du ZQ and Yang CX (2018). Reduced nucleic acid methylation impairs meiotic maturation and developmental potency of pig oocytes. *Theriogenology* **121**, 160–7.

Wu R, Liu Y, Zhao Y, Bi Z, Yao Y, Liu Q, Wang F, Wang Y and Wang X (2019). m^6A methylation controls pluripotency of porcine induced pluripotent stem cells by targeting SOCS3/JAK2/STAT3 pathway in a YTHDF1/YTHDF2-orchestrated manner. *Cell Death Dis* **10**, 171.

Xia H, Zhong C, Wu X, Chen J, Tao B, Xia X, Shi M, Zhu Z, Trudeau VL and Hu W (2018). Mettl3 Mutation disrupts gamete maturation and reduces fertility in zebrafish. *Genetics* **208**, 729–43.

Xu Q and Xie W (2018). Epigenome in Early mammalian development: inheritance, reprogramming and establishment. *Trends Cell Biol* **28**, 237–53.

Yang XQ, Wu ZF and Li ZC (2019). Advances in epigenetic reprogramming of somatic cells nuclear transfer in mammals. *Yi Chuan* **41**, 1099–109.

Yartseva V and Giraldez AJ (2015). The maternal-to-zygotic transition during vertebrate development: a model for reprogramming. *Curr Top Dev Biol* **113**, 191–232.

Zhao BS, Wang X, Beadell AV, Lu Z, Shi H, Kuuspalu A, Ho RK and He C (2017). m^6A-dependent maternal mRNA clearance facilitates zebrafish maternal-to-zygotic transition. *Nature* **542**, 475–78.

Zhou W, Niu YJ, Nie ZW, Kim JY, Xu YN, Yan CG and Cui XS (2020). Nuclear accumulation of pyruvate dehydrogenase alpha 1 promotes histone acetylation and is essential for zygotic genome activation in porcine embryos. *Biochim Biophys Acta Mol Cell Res* **1867**, 118648.

https://doi.org/10.1017/S0967199420000799 Published online by Cambridge University Press